Fuel 256 (2019) 115914

Contents lists available at ScienceDirect

Fuel

journal homepage: www.elsevier.com/locate/fuel

Full Length Article

Effects of water vapor and temperature on NO_x and CO emissions during converter gas combustion

Yinghua Zhai[a,b], Sen Li[a,c,*], Weiping Yan[b], Xiaolin Wei[a,c], Leyu Zhang[a], Youtian Wang[b]

[a] State Key Laboratory of High Temperature Gas Dynamics, Institute of Mechanics, Chinese Academy of Sciences, Beijing 100190, China
[b] North China Electric Power University, Baoding, Hebei Province 071000, China
[c] Dalian National Laboratory for Clean Energy, Dalian 116023, China

ARTICLE INFO

Keywords:
Water vapor concentration
Converter gas
Inlet temperature
CO emission
NO emission

ABSTRACT

Converter gas is a valuable fuel in the converter steelmaking process, and NO_x and CO emissions are high due to the high temperature combustion and the absence of H_2O vapor. The effects of H_2O vapor concentration and the inlet temperature of converter gas on NO_x and CO emissions in the combustion are investigated by a detailed chemical reaction mechanism. CO emission decreases sharply when $C_{H2O,inlet}$ increases from 0 to 0.4%. At $C_{H2O,inlet} > 0.4\%$ and $T_{inlet} < 950$ K, for the reduction of CO emission, the inlet temperature of converter gas is predominant over that of H_2O vapor in air. The inlet temperature of converter gas has noticeable influence on NO emission at $C_{H2O,inlet} < 2\%$. With the increase of $C_{H2O,\ inlet}$, NO emission first increases, then reaches a peak value, finally decreases. At $T_{inlet} > 1050$ K and $C_{H2O,inlet} > 2\%$, NO emission noticeably decreases with $C_{H2O,inlet}$. In the presence of H_2O, H and OH free radicals are easily formed, the reduction path of NO is as follows: NO → NH/HNO → N_2.

1. Introduction

After more than 60 years of steelmaking development, oxygen converter steelmaking is generally divided into top-blowing, bottom-blowing and mixed-blowing types [1,2]. One of the characteristics of oxygen converter steelmaking is the production of converter gas. Converter gas is a valuable fuel containing ~80% carbon monoxide (CO) with high temperature (800–1900 K), but NO_x and CO emissions are high in the combustion due to the high temperature combustion and the absence of H_2O vapor [3].

Pin-Wei Li et al. [4] studied NO_x emissions in fluidized bed combustion, they found that lowering bed temperature by water addition could reduce NO_x formation. Farooq Sher et al. [5–7] studied the effect of air staging at different injection locations on NO_x emissions of utility boiler, and the injection of the secondary air at the high location was conducive to reduce NO_x emissions. Daniel Pugh et al. [8] found that free radical OH accelerated the oxidation of CO. Thus, the reduction of NO_x and CO emissions in combustion system is a complex process involving flow mix and chemical reaction.

For converter flue gas containing ~80% CO, and increasing the burnout efficiency of CO is more important at present, which makes CO_2 capture become easy to avoid the global warming [9,10]. In order to reduce CO and NO_x emissions during converter flue gas combustion, Sen Li et al. [11,12] simulated the high-temperature converter gas combustion by using the counter flow diffusion flame model with a detailed chemical reaction mechanism, they found that NO_x emissions were related to air stoichiometric ratio and gas temperature, and the air supply mode must be improved to effectively organize the mixing of off-gas and air in the cooling stack. Le Cong T [13] and Huaming Dai et al. [14] pointed out that water vapor inhibited the oxidation of hydrogen and methane. Sen Li et al. [15] found that water vapor was crucial to converter gas combustion, and the water vapor content in air was very important in converter gas combustion system.

In steelmaking converter flue gas, water vapor concentration is 0, water vapor content in air used in the combustion system is low, and water vapor can't be produced in the converter gas combustion. Therefore, in order to improve the combustion efficiency of converter gas, a certain amount of water vapor must be added in air. At present, there are few reports about the effect of water vapor content of air on CO and NO_x emissions in converter gas combustion.

In order to realize high-efficient and clean combustion of converter gas, the effects of water vapor and temperature on NO_x and CO emissions are investigated in the study. Non-premixed combustion of high-temperature converter gas by adding water vapor in air is studied by a detailed chemical reaction mechanism, the effects of water vapor concentration in air (0–5%) and converter gas temperature (823–1153 K)

* Corresponding author at: Institute of Mechanics, Chinese Academy of Sciences, Beijing 100190, China.
E-mail address: lisen@imech.ac.cn (S. Li).

https://doi.org/10.1016/j.fuel.2019.115914
Received 4 April 2019; Received in revised form 18 July 2019; Accepted 26 July 2019
Available online 07 August 2019
0016-2361/

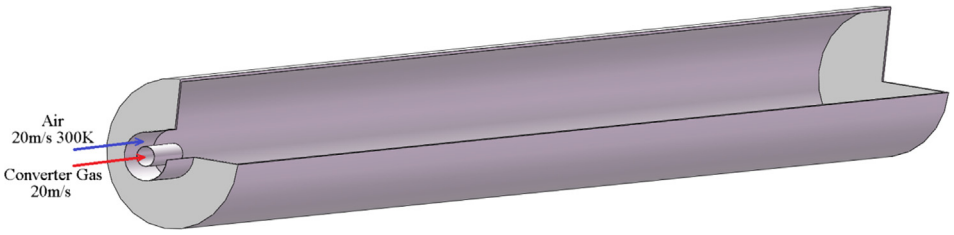

Fig. 1. Schematic of simulated combustion furnace.

on CO and NO emissions are investigated, and the reaction paths of CO oxidization and NO formation are analyzed.

2. Simulation model of converter gas combustion

2.1. Physical models

In the study, in order to prevent explosion and backfire, a typical combustion device model with the turbulent non-premixed combustion of coaxial jet is used. The combustion device is cylindrical furnace with a length of 500 mm and a diameter of 50 mm, which is shown in Fig. 1. A co-flow burner is adopted, the inlet inner diameter of converter gas is 6.8 mm, air is fed into the furnace through an annular inlet, and the inner diameter and outer diameter of the annular inlet are respectively 6.8 mm and 16.8 mm. In the simulation, Reynolds number (*Re*) of the flue gas in the furnace is above 10^4, and the combustion belongs to turbulent diffusion combustion.

Due to the symmetry of physical model and operating conditions, a two-dimensional model is used to simulate the combustion. The grid is a two-dimensional structural grid with sufficient grid independence to satisfy 4999 × 248 grid nodes (1234506 units). The boundary operating conditions are presented in Table 1.

2.2. Combustion model

A non-premixed laminar flamelet model is used to simulate the turbulent flame. The laminar flamelet is included in the turbulent flame using the static Probability Density Function (PDF) method [16]. For adiabatic systems, the species mass fraction in the laminar flamelet is completely parameterized by f and χ_{st}, mean species mass fraction and temperature in the turbulent flame can be determined from the PDF of f and χ_{st} as [17]

$$\bar{\phi} = \int\int \phi(f,\chi_{st})p(f,\chi_{st})df d\chi_{st}$$

where ϕ is a representative scalar, such as a species mass fraction, temperature, or density.

$$\chi_{st} = \frac{a_s \exp(-2[\mathrm{erfc}^{-1}(2f_{st})]^2)}{\pi}$$

where χ_{st} – scalar dissipation at $f = f_{st}$; a_s – characteristic strain rate; f_{st} – stoichiometric mixture fraction; erfc^{-1} – inverse complementary error function.

In the non-premixed combustion model, the turbulent diffusion flame is considered as an ensemble of laminar flamelets, and chemical reactions and heat transfer occur in a thin layer [18]. The combustion of converter gas usually occurs in the flamelet region of turbulent combustion, which makes the flame model suitable for turbulent diffusion flames [19,20]. To take into account the turbulence effects, the realizable standard k–ε turbulence model is used [21,22].

Table 1
Boundary operating conditions [1].

Concentration of the converter gas			Gas inlet velocity	Air inlet velocity	Excess air coefficient	Converter gas temperature
65% CO	34% CO_2	1% N_2	20 m/s	20 m/s	1.05	823–1153 K

2.3. Model validation

In the combustion simulation, a detailed chemical reaction mechanism containing 114 elemental reactions of 37 components is adopted [23]. In order to validate the detailed mechanism, the moist CO combustion experiment was performed by Allen in a large diameter flow reactor, the initial mole fractions of CO and H_2O were 5.8×10^{-3} and 1.1×10^{-4}, respectively. The experimental results were compared with the simulation results, and the results were in good agreement with each other, as shown in Fig. 2 [23].

3. Result and discussion

3.1. Effects of water vapor concentration and the inlet temperature of the converter gas on CO emission

The influences of inlet temperature (T_{inlet}) of converter gas and water vapor concentration ($C_{H2O,inlet}$) in air on the CO emission are studied, and the result is shown in Fig. 3. $C_{CO,outlet}$, and $C_{NO,outlet}$ are the mean concentrations of CO and NO at the furnace outlet. $C_{CO,outlet}$ decreases sharply when $C_{H2O,inlet}$ increases from 0 to 0.4%, but the effect of $C_{H2O,inlet}$ on the CO emission is negligible at $C_{H2O,inlet} > 0.4\%$. The result indicates that water vapor has significant promoting effect on CO oxidization by increasing $C_{H2O,inlet}$ when $C_{H2O,inlet}$ is too low. At $C_{H2O,inlet} > 0.4\%$ and $T_{inlet} < 950$ K, for CO oxidization, T_{inlet} is predominant over $C_{H2O,inlet}$, and increasing temperature can effectively improve CO oxidization (see Fig. 3).

3.1.1. Effect of water vapor concentration in air on CO emission

Fig. 4 shows CO oxidization reaction pathways in the absence/presence of H_2O, where flame temperature reaches the maximum value

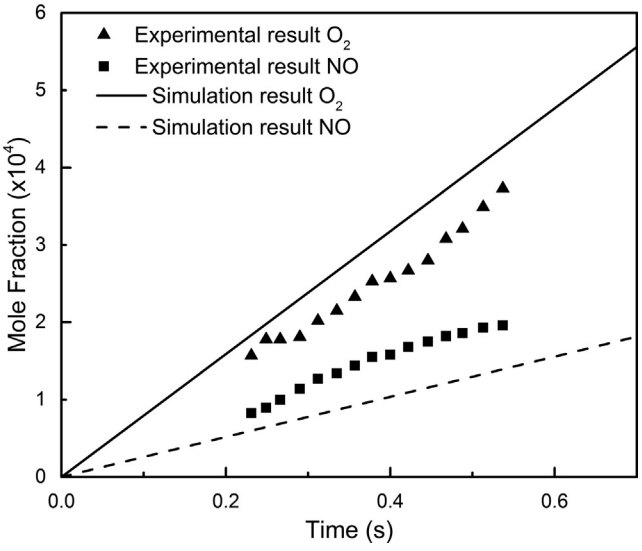

Fig. 2. Comparison between experiment and simulation results [23].

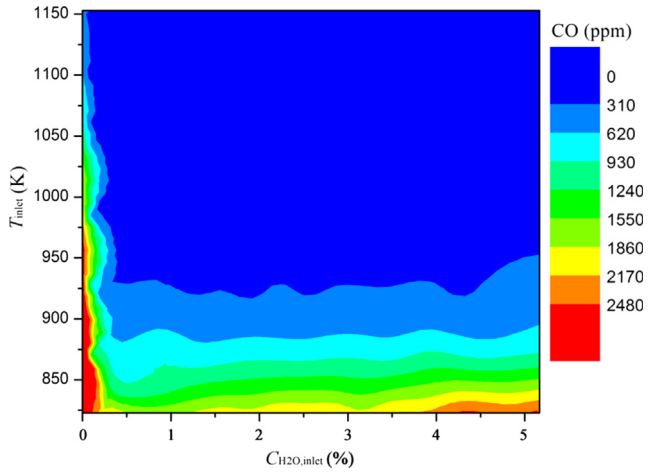

Fig. 3. Effects of $C_{H2O,inlet}$ and T_{inlet} on CO emission.

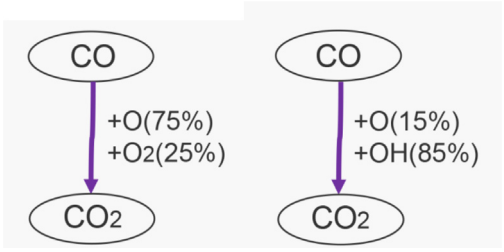

(a) In the absence of H_2O (b) In the presence of H_2O

Fig. 4. Schematic diagram of reaction pathways for CO.

at the centerline of furnace. In the absence of H_2O, CO reacts directly with the O free radical and O_2 to form CO_2, the contribution rates of O and O_2 in the CO oxidization reactions are respectively 75% and 25% (see Fig. 4a), and the corresponding chemical reaction equations are as R1 and R2:

$$CO + O\cdot = CO_2 \quad (R1)$$

$$CO + O_2 = CO_2 + O\cdot \quad (R2)$$

O free radical is only formed at high temperature, the reaction rate is low, thus CO is difficult to be combusted completely in the absence of H_2O.

In the presence of H_2O, CO oxidization mainly depends on the following reactions:

$$H_2O = H\cdot + OH\cdot. \quad (R3)$$

$$CO + OH\cdot = CO_2 + H\cdot \quad (R4)$$

H_2O is decomposed to generate OH free radical, OH plays a very important role in CO combustion, and CO is more easily oxidized by OH than O (see Fig. 4b).

Fig. 5 shows the effect of $C_{H2O,inlet}$ on the distribution of OH free radical in flame at T_{inlet} = 873 K. In Fig. 5, *d* represents the furnace diameter, *R* represents the furnace radius, *X* represents furnace length, and *X/d* and *R/d* represents dimensionless dimension. The results indicate that OH concentration obviously increases with the increase of $C_{H2O,inlet}$. The concentration profiles of OH free radical at the centerline of the furnace are plotted in Fig. 6 at $C_{H2O,inlet}$ = 0.06–0.32% and T_{inlet} = 923 K. With the increase of $C_{H2O,inlet}$ from 0.06% to 0.32%, and the maximum value of OH concentration increases from 244 ppm to 584 ppm. Therefore, increasing $C_{H2O,inlet}$ can accelerate CO oxidation by providing sufficient OH free radical (see R3 and R4), and CO emission sharply decreases with the increase of $C_{H2O,inlet}$ (see Fig. 3) at $C_{H2O,inlet}$ < 0.4%. Thus, OH free radical assists complete combustion of

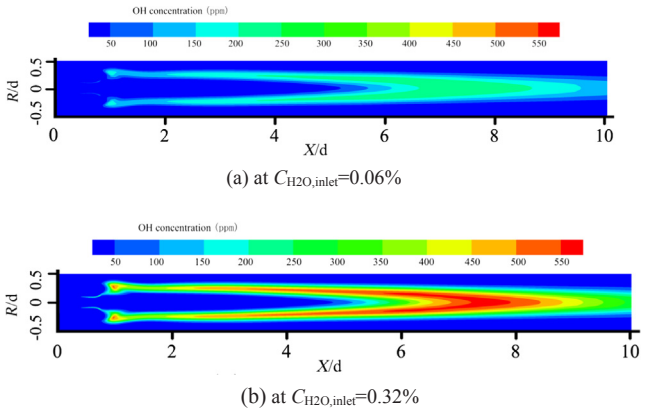

Fig. 5. Distributions of OH concentration in the furnace.

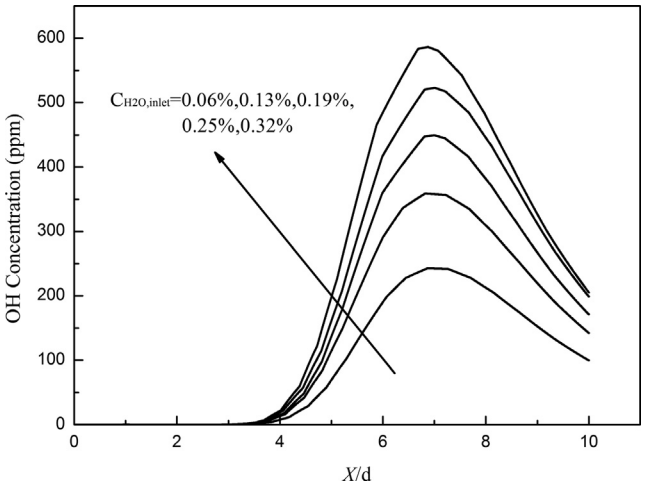

Fig. 6. The profiles of OH concentration at the centerline of furnace at different $C_{H2O,inlet}$.

CO, and CO emission finally decreases. As known from Fig. 6, the increase of OH concentration slows down at higher $C_{H2O,inlet}$, OH free radical reaches equilibrium state (see R3), thus effect of $C_{H2O,inlet}$ on the CO emission is negligible at $C_{H2O,inlet}$ > 0.4% (see Fig. 3).

3.1.2. *Effect of the inlet temperature of the converter gas on CO emission*

Fig. 7 shows the effect of T_{inlet} on CO distribution in furnace at $C_{H2O,inlet}$ = 2%. As compared to CO combustion at T_{inlet} = 988 K, the burnout of CO is delayed at T_{inlet} = 823 K. The increase of combustion temperature can induce a large amount of OH free radical in flame [24].

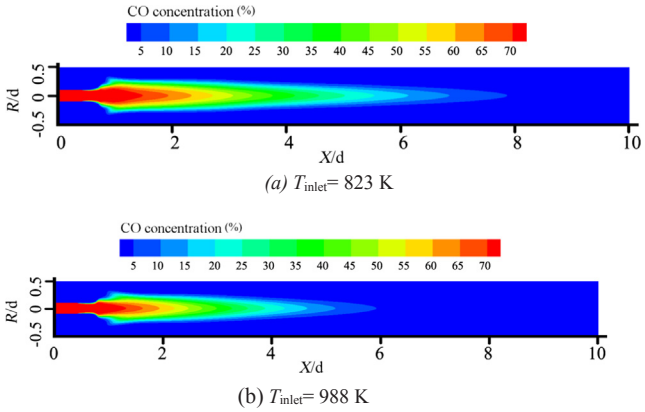

Fig. 7. Distributions of CO concentration in the furnace.

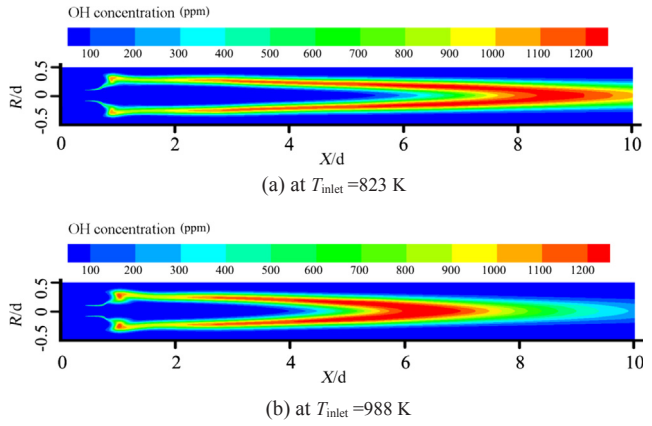

Fig. 8. Distributions of OH free radical.

The distribution of OH free radical in flame at T_{inlet} = 823 K and 988 K is provided in Fig. 8.

Increasing T_{inlet} accelerates the reaction rate of CO oxidization (see R4), OH free radical is rapidly consumed. Thus the distribution of OH free radical obviously shrinks when T_{inlet} increases in Fig. 8. OH free radical concentration at the centerline of furnace is provided in Fig. 9 at $C_{H2O,inlet}$ = 2% and T_{inlet} = 823–988 K.

Fig. 9 shows the profiles of OH concentration at the centerline of the furnace at different T_{inlet}. The result indicates that T_{inlet} has no significant effect on the maximum concentration of OH free radical. With the increase of T_{inlet}, the maximum concentration of OH radical just increases slightly, and the location of X/d corresponding to the peak value of the OH free radical at the centerline of the furnace decreases. The results mean that the height of the flame is lowered, and increasing temperature accelerates CO combustion and results in the decrease of the flame height.

Fig. 10 shows the effect of T_{inlet} and $C_{H2O,inlet}$ on the flame surface height. Based on the highest OH radical concentration at the centerline of the furnace, the flame surface height (H_f) is obtained [20].

Flame height increases with the increase of $C_{H2O,inlet}$ at a given T_{inlet}, and it decreases noticeably with the increase of T_{inlet} (see Fig. 10). With the increase of $C_{H2O,inlet}$, the increase of flame height and OH concentration enlarges combustion reaction zone and enhances CO oxidization rate (see R4), thus CO emission is reduced (see Fig. 3). The increase of T_{inlet} accelerates the reaction rate of CO oxidization (see R4), OH free radical is rapidly consumed, flame height decreases (see Fig. 10), and CO emission is reduced (see Fig. 3).

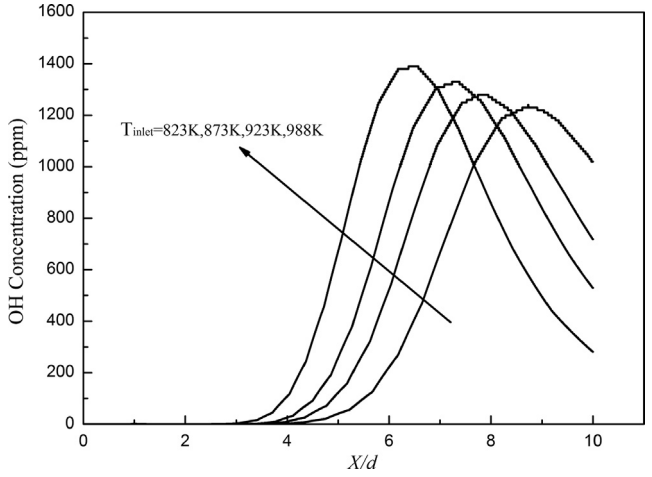

Fig. 9. The profiles of OH concentration at the centerline of furnace at different T_{inlet}.

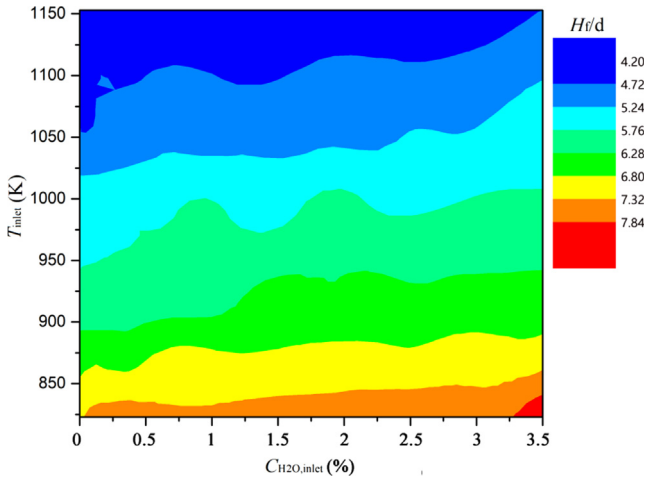

Fig. 10. Effects of $C_{H2O,inlet}$ and T_{inlet} on flame height (where, H_f/d represents dimensionless dimension).

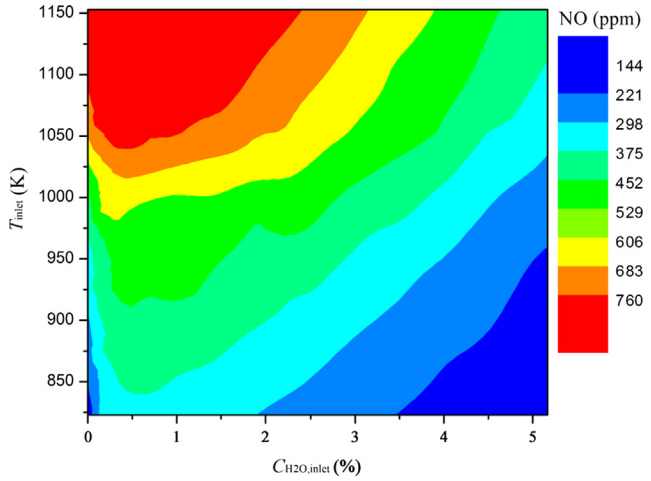

Fig. 11. Effects of $C_{H2O,inlet}$ and T_{inlet} on NO emission.

3.2. Effects of water vapor concentration and converter gas temperature on NO emission

Fig. 11 shows the effects of $C_{H2O,\ inlet}$ and T_{inlet} on NO emission. NO emission increases gradually with the increase of T_{inlet}, and T_{inlet} has noticeable influence on NO emission at $C_{H2O,inlet}$ < 2%. With the increase of $C_{H2O,inlet}$, NO emission first increases, then reaches a peak value, finally decreases. With the increase of T_{inlet}, the occurrence location of the peak value moves to low $C_{H2O,\ inlet}$, and the peak value increases. At T_{inlet} > 1050 K and $C_{H2O,inlet}$ > 2%, NO emission noticeably decreases with $C_{H2O,inlet}$.

Fig. 12 shows the effects of $C_{H2O,\ inlet}$ and T_{inlet} on the maximum flame temperature, and the results are similar to those of NO emission (see Fig. 11). The maximum flame temperature increases gradually with the increase of T_{inlet}. With the increase of $C_{H2O,inlet}$, the maximum flame temperature first increases, then reaches a peak value, and finally decreases. With the increase of T_{inlet}, the occurrence location of the peak value moves to low $C_{H2O,\ inlet}$, and the peak value increases.

The influence similarity of $C_{H2O,inlet}$ and T_{inlet} on NO emission and the maximum flame temperature indicates that, $C_{H2O,inlet}$ and T_{inlet} directly influence flame temperature and result in the variation of thermal-NO formation, thus the increase of T_{inlet} and the decrease of $C_{H2O,inlet}$ promote thermal-NO formation and result in the increase of NO emission (see Fig. 11). At $C_{H2O,inlet}$ < 2%, T_{inlet} has noticeable influence on maximum flame temperature(see Fig. 12), because water

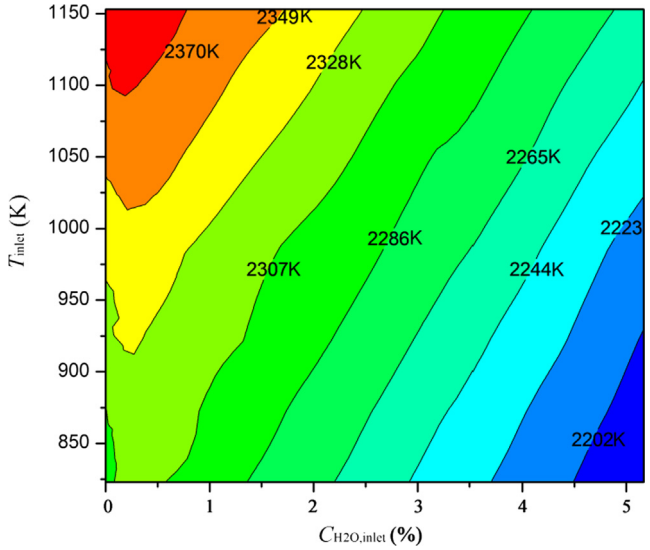

Fig. 12. Effects of $C_{H2O,inlet}$ and T_{inlet} on the maximum flame temperature.

vapor concentration is low, the concentration of OH radical is low, the flame is prone to local high temperature. Thus, T_{inlet} has noticeable influence on NO emission at $C_{H2O,inlet} < 2\%$ (see Fig. 11).

The variation of flame temperature influenced by $C_{H2O,inlet}$ and T_{inlet} effects OH free radical formation and CO oxidization (see R3 and R4), thus CO emission decreases with the increase of $C_{H2O,inlet}$ and T_{inlet} (see Fig. 3).

At $T_{inlet} = 1103$ K, the profiles of the main species at the centerline of the furnace are shown in Fig. 13 and Fig. 14 at $C_{H2O,inlet} = 0$ and 0.9%.

Figs. 13 and 14 show the profiles of the main species at the centerline of the furnace at $C_{H2O,inlet} = 0$ and 0.9%, respectively. At $C_{H2O,inlet} = 0$, the main intermediate species is only O free radical. At $C_{H2O,inlet} = 0.9\%$, a large number of intermediate species are formed, such as H, OH, and HNO. The reaction path diagrams of NO formation in the absence/presence of H_2O are respectively provided in Fig. 15, where flame temperature reaches maximum value at the centerline of furnace.

As shown in Fig. 15(a), in the absence of H_2O, the corresponding chemical reaction paths of NO_x formation are as follows:

$$N_2 + O_2 = N_2O + O\cdot \quad \text{(R5)}$$

$$N_2 + O\cdot = N_2O \quad \text{(R6)}$$

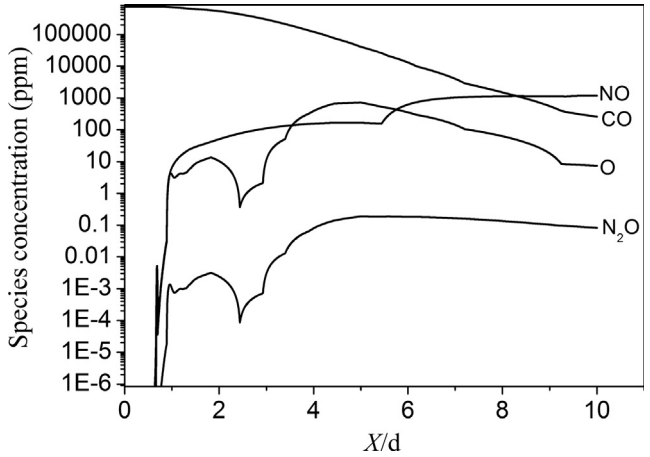

Fig. 13. Concentration profiles of the main species at the centerline of the furnace in the absence of water vapor.

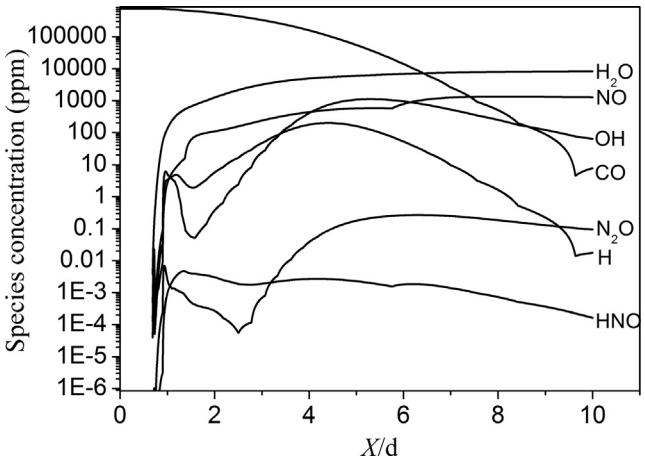

Fig. 14. Concentration profiles of the main species at the centerline of the furnace at $C_{H2O,inlet} = 0.9\%$.

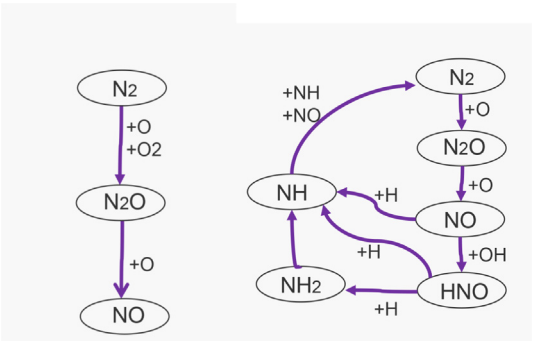

(a) In the absence of H_2O (b) In the presence of H_2O

Fig. 15. Schematic diagram of reaction pathways for NO formation/reduction.

$$N_2O + O\cdot = NO + NO \quad \text{(R7)}$$

N_2 reacts with O_2 and O to form N_2O, then N_2O reacts with O to form NO. Different from NO formation mechanism proposed by Zeldovich [25,26], the intermediate species N_2O is produced because of the high temperature in the converter (~2370 K, see Fig. 12).

As shown in Fig. 15(b), in the presence of H_2O, the corresponding chemical reaction equations are R3, R8-R14.

$$NO + H\cdot = NH\cdot + O\cdot \quad \text{(R8)}$$

$$NO + OH\cdot = HNO\cdot + O\cdot \quad \text{(R9)}$$

$$HNO\cdot + H\cdot = NH\cdot + OH\cdot \quad \text{(R10)}$$

$$HNO\cdot + H\cdot = NH_2\cdot + O\cdot \quad \text{(R11)}$$

$$NH_2\cdot + H\cdot = NH\cdot + H_2 \quad \text{(R12)}$$

$$NH\cdot + NH\cdot = N_2 + H\cdot + H\cdot \quad \text{(R13)}$$

$$NH\cdot + NO = N_2 + OH\cdot \quad \text{(R14)}$$

Due to the presence of H_2O, a lot of H and OH free radicals are formed, a large amount of NO is transformed into NH, HNO radicals, and HNO radical is converted to NH and NH_2 radicals and finally to N_2. Therefore, H free radical can reduce NO emission. This result is very similar to that of Sen Li's previous study. In Sen Li's study, in the presence of H_2O, the formation of free-radical H is conducive to NO reduction. H_2O has a complex effect on NO emission: at $T < 1100$ °C, NO emission decreases with the increase of H_2O content [15]. Thus, increasing $C_{H2O,inlet}$ is conducive to reduce NO emission.

4. Conclusions

To realize high-efficient and clean combustion of converter gas, the non-premixed combustion of high-temperature converter gas by adding water vapor in air was simulated by the detailed chemical reaction mechanism, the effects of water vapor concentration and converter gas temperature on CO and NO emissions were investigated, and the reaction paths of CO oxidization and NO formation were provided. The following conclusions are drawn:

(1) At $C_{H2O,inlet}$ = 0–0.4%, H_2O vapor has significant influence on CO combustion, and CO emission decreases with the increase of $C_{H2O,inlet}$; at $C_{H2O,inlet}$ > 0.4% and T_{inlet} < 950 K, CO emission noticeably decreases with the increase of T_{inlet}; at $C_{H2O,inlet}$ < 2%, NO emission rapidly increases with T_{inlet}; at T_{inlet} > 1050 K and $C_{H2O,inlet}$ > 2%, NO emission noticeably decreases with $C_{H2O,inlet}$.
(2) In the presence of H_2O vapor, CO is more easily oxidized by OH than O, OH easily reaches an equilibrium with the increase of T_{inlet}, a large amount of NO is transformed into NH, HNO radicals, HNO radical is converted to NH and NH_2 radicals, and NO is finally reduced to N_2.

Based on the study, in the practical application, the reasonable adjustment of $C_{H2O,\ inlet}$ and T_{inlet} can effectively reduce CO and NO_x emissions, and high-efficient and clean combustion of converter gas can be realized.

Acknowledgements

This work was supported by the “Transformational Technologies for Clean Energy and Demonstration”, Strategic Priority Research Program of the Chinese Academy of Sciences, Grant No. XDA21040500.

References

[1] Li Sen, Wei Xiaolin, Yu Lixin. Numerical simulation of off-gas formation during top-blown oxygen converter steelmaking. Fuel 2011;90(4):1350–60. https://doi.org/10.1016/j.fuel.2011.01.022.
[2] Aleksashin AL, Schnaltzger I, Hollias G. Creation and growth of oxygen-converter steelmaking. Metallurgist 2007;51(1–2):60–5. https://doi.org/10.1007/s11015-007-0014-4.
[3] Perlov N, Nitskevich E. Efficient use of converter gas. Metallurgist 1965;9(3):149–51.
[4] Li Pin-Wei, Chyang Chien-Song. A comprehensive study on NO_x emission and fuel nitrogen conversion of solid biomass in bubbling fluidized beds under staged combustion. J Energy Inst 2019. https://doi.org/10.1016/j.joei.2019.02.007.
[5] Sher, Farooq, et al. Experimental investigation of woody and non-woody biomass combustion in a bubbling fluidised bed combustor focusing on gaseous emissions and temperature profiles. Energy 2017;141:2069–80. https://doi.org/10.1016/j.energy.2017.11.118.
[6] Sher, Farooq, et al. Oxy-fuel combustion study of biomass fuels in a 20 kWth fluidized bed combustor. Fuel 2018;215:778–86. https://doi.org/10.1016/j.fuel.2017.11.039.
[7] Zhang Yong, et al. Effect of slot wall jet on combustion process in a 660 MW opposed wall fired pulverized coal boiler. Int J Chem Reactor Eng 2019;17(4). https://doi.org/10.1515/ijcre-2018-0110.
[8] Daniel Pugh, et al. Catalytic influence of water vapor on lean blow-off and NO_x reduction for pressurized swirling syngas flames. J Eng Gas Turbines Power 2018;140(6):061502https://doi.org/10.1115/1.4038417.
[9] Sher, Farooq, et al. Sustainable energy saving alternatives in small buildings. Sustainable Energy Technol Assessments 2019;32:92–9. https://doi.org/10.1016/j.seta.2019.02.003.
[10] Cuce, Erdem, et al. Strategies for ideal indoor environments towards low/zero carbon buildings through a biomimetic approach. Int J Ambient Energy 2019;40(1):86–95. https://doi.org/10.1080/01430750.2017.1372807.
[11] Li Sen, Wei Xiaolin. Numerical simulation of CO and NO emissions during converter off-gas combustion in the cooling stack. Combust Sci Technol 2013;185(2):212–25. https://doi.org/10.1080/00102202.2012.715606.
[12] Li Sen, Wei Xiaolin, Yu Linxin. Numerical study on NO_x/CO emissions in the diffusion flames of high-temperature off-gas of steelmaking converter. Appl Energy 2011;88(4):1113–9. https://doi.org/10.1016/j.apenergy.2010.10.030.
[13] Le Cong T, Dagaut P. Experimental and detailed modeling study of the effect of water vapor on the kinetics of combustion of hydrogen and natural gas, impact on NO_x. Energy Fuels 2009;23(2):725–34.
[14] Dai Huaming, Zhao Qi, Lin Baiquan, He Song, Chen Xianfeng, Zhang Ying, et al. Premixed combustion of low-concentration coal mine methane with water vapor addition in a two-section porous media burner. Fuel 2018;213:72–82. https://doi.org/10.1016/j.fuel.2017.09.123.
[15] Li Sen, Wei Xiaolin, Guo Xiaofeng. Effect of H_2O vapor on NO reduction by CO: experimental and kinetic modeling study. Energy Fuels 2012;26(7):4277–83.
[16] Chen JY, Kollmann W, Dibble RW. Pdf modeling of turbulent nonpremixed methane jet flames. Combust Sci Technol 1989;64(4–6):315–46.
[17] Fluent, A. N. S. Y. S., Ansys fluent theory guide, ANSYS Inc., USA 15317 (2011) 724–746.
[18] LiSen, et al. Mixing and combustion modeling of hydrogen peroxide/kerosene shear-coaxial jet flame in lab-scale rocket engine. Aerospace Sci. Technol. 2016;56:148–54. https://doi.org/10.1016/j.ast.2016.07.008.
[19] Dai H, Lin B. Scale effect of ceramic foam burner on the combustion characteristics of low-concentration coal mine methane. Energy Fuels 2014;28(10):6644–54.
[20] Vervisch L, Poinsot T. Direct numerical simulation of non-premixed turbulent flames. Annu Rev Fluid Mech 1998;30(1):655–91. https://doi.org/10.1146/annurev.fluid.30.1.655.
[21] Stapleton KW, et al. On the suitability of k–ε turbulence modeling for aerosol deposition in the mouth and throat: a comparison with experiment. J Aerosol Sci 2000;31(6):739–49. https://doi.org/10.1016/S0021-8502(99)00547-9.
[22] Murakami, Shuzo. Overview of turbulence models applied in CWE–1997. J Wind Eng Ind Aerodyn 1998;74:1–24. https://doi.org/10.1016/S0167-6105(98)00004-X.
[23] Allen MT, Yetter RA, Dryer FL. High pressure studies of moist carbon monoxide/nitrous oxide kinetics. Combust Flame 1997;109(3):449–547. https://doi.org/10.1016/S0010-2180(96)00181-2.
[24] Aizawa T, Kamimoto T, Tamaru T, Measurements of temperature and OH radical concentration in combustion gases by absorption spectroscopy with a diode laser, Technical Digest, CLEO/Pacific Rim'99. Pacific Rim Conference on Lasers and Electro-Optics (Cat. No. 99TH8464). IEEE, 2 (1999) 567-568.
[25] Bowman Craig T. Kinetics of pollutant formation and destruction in combustion. Prog. Energy Combustion Sci. 1975;1(1):33–45. https://doi.org/10.1016/0360-1285(75)90005-2.
[26] Zeldovich, Ya B, Ya Sadovnikov P, Frank-Kamenetskii DA. Oxidation of Nitrogen in Combustion, translation by M., Shelef, Academy of Sciences of USSR, Institute of Chemical Physics, Moscow-Leningrad (1947).